Supplementary Data

Insights into the Structure and Assembly of the *Bacillus subtilis* Clamp-Loader Complex and its Interaction with the Replicative Helicase

José P. Afonso,[1] Kiran Chintakayala,[2] Chatrudee Suwannachart,[3] Svetlana Sedelnikova,[3] Kevin Giles,[4] John B. Hoyes,[4] Panos Soultanas,[2] John Rafferty,[3] and Neil J. Oldham[1,*]

[1]School of Chemistry, University of Nottingham, University Park, Nottingham NG7 2RD, UK

[2]School of Chemistry and Centre of Biomolecular Sciences, University of Nottingham, University Park, Nottingham NG7 2RD, UK

[3]Department of Molecular Biology and Biotechnology, University of Sheffield, Firth Court, Western Bank, Sheffield S10 2TN, UK

[4]Waters Corporation, Floats Road, Manchester, M23 9LZ, UK

*Correspondence: neil.oldham@nottingham.ac.uk; tel: +44 (0)115 9513542; fax: +44 (0)115 9513564

Experimental Procedures

Mass Spectrometry-Ion Mobility Spectrometry. IMS measurements were performed to obtain the drift times for the clamp-loader and three calibrant proteins of known collisional cross section (CCS) (1), namely transthyretin, alcohol dehydrogenase and glutamate dehydrogenase (Sigma). IMS was conducted using the Water Synapt HDMS described in the Experimental Procedures of the main paper with the following additional parameters: nitrogen was used as the IM gas and all proteins were analysed at a wave height of 10 V, wave velocity of 300 $m.s^{-1}$ and IM gas flow of 30.0 $mL.min^{-1}$. Collisional energies were 30 V in the trap and 20 V in the transfer and the trap gas flow was 6.0 $mL.min^{-1}$. To calculate the CCS of the clamp-loader, a calibration was made from data obtained for the three calibrant proteins, using a method described elsewhere (2)

The CCS of the obtained model was theoretically estimated by the projection approximation method (PA) using Driftscope 2.1 software (Waters, Manchester, UK), scaled by the empirical correction factor (x 1.14) determined by Bush *et al.* (3) and compared with the experimental CCS.

Molecular Dynamics Simulations. The *Bacillus subtilis* clamp-loader homology model was subjected to gas-phase MD simulation using the Amber99SB force field operating on the European eNMR grid (4). Prior to MD simulations, subunit structures were relaxed by 10,000 steps of energy minimization in the gas phase at 300 K (Amber 11 Sander parameters: imin=1, maxcyc=10000, ncyc= 5000, ntb=0, cut=12.0, igb=0; all other parameters sander defaults). Each subunit was then subjected to MD simulation in the gas phase for 100 ps at 300 K (Amber 11 Sander parameters: imin=0, ntb=0, cut=12.0, igb=0, ntt=3, gamma ln=1, temp0=300, tempi=300, nstlim=100000, ntpr=1000, ntwx=1000; all other parameters sander defaults). The final output structures were realigned using Hex (5) and displayed using Pymol (6).

X-ray Crystallography. The primers used to clone yqeN (δ) from *Bacillus subtilis* genomic DNA are given in Table S1.

Table S1. Primers used for *yqeN* cloning from genomic DNA.

Name	DNA Oligonucleotide Sequence
*yqeN-Nco*I-F	5'-GTCGTACAACACCATGGTATTTGATGTGTGGA-3'
*yqeN-Bam*HI-R	5'-AAAACGATCCGGATCCTTAATAATGGGGATCG-3'
*hol*B-*Eco*RV-F	5'- AGAGTGATACAGATATCATGGCAATATCCTGG-3'
*hol*B-*Xho*I-R	5'- ATTGTACAAGCCTCGAGTTATCCCTCCTGCAA-3'

Results

Ion Mobility. Calibration of the travelling wave ion mobility (TWIM) cell of the Waters Synapt using the procedure described by Ruotolo et al. (2), and the literature CCS values measured by Bush *et al.* (1) yielded the curves shown in Fig S1 and Fig S2. The three calibrant proteins employed bracketed the CCS for the clamp loader complex. CCS values ranging from 10418 to 10879 $Å^2$ were measured for clamp loader according to the charge state (see Fig. S3).

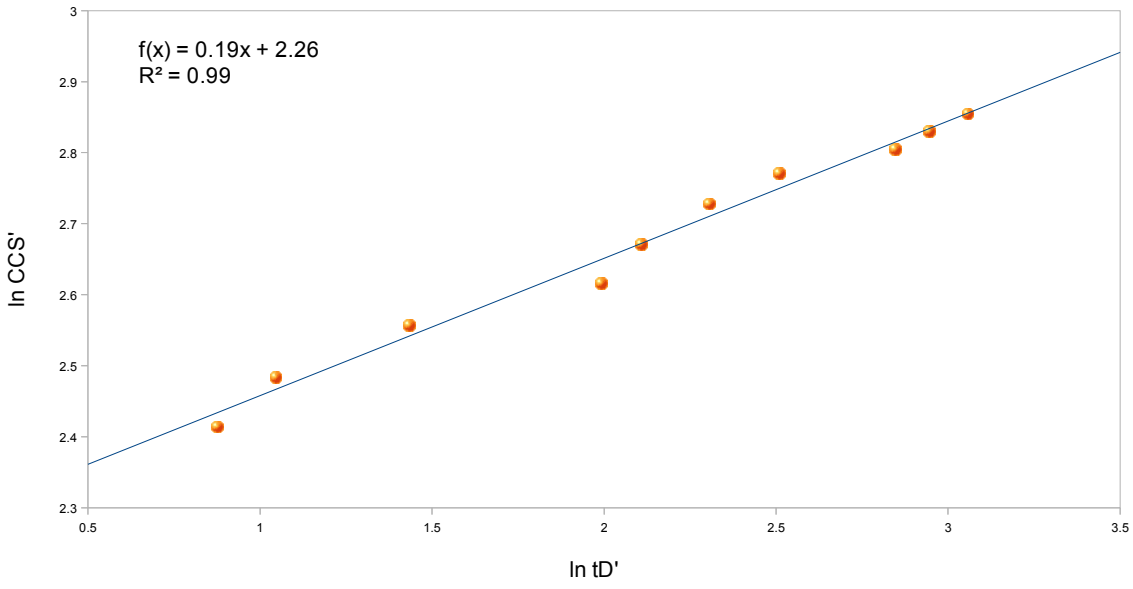

Figure S1. Plot of ln t_D' against ln CCS′ yielding a value for the gradient m of 0.19. See (2) for method.

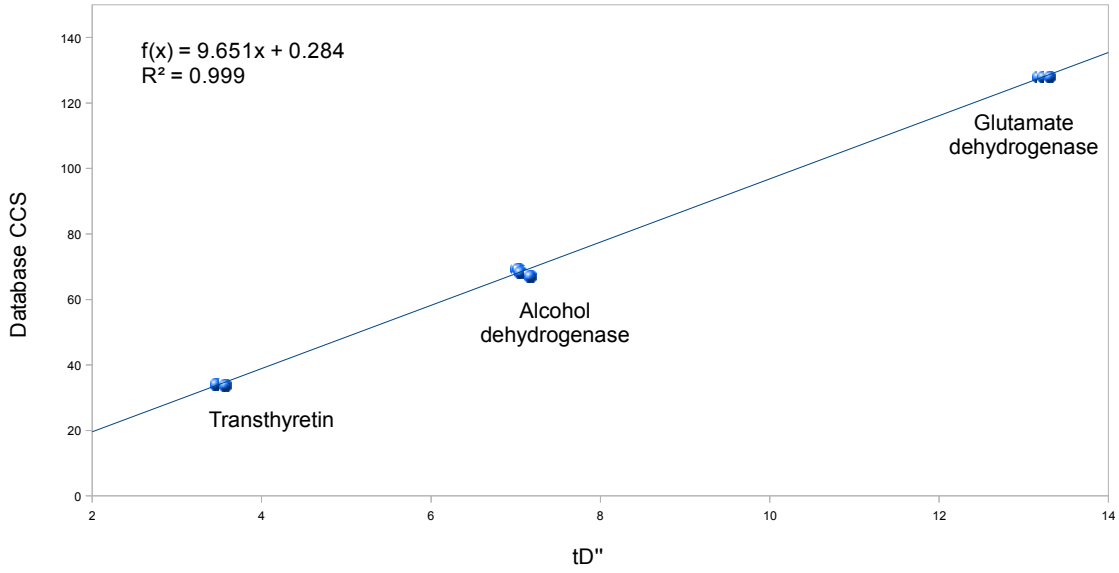

Figure S2. Plot of tD″ against the database CCS values (1) for transthyretin, alcohol dehydrogenase, and glutamate dehydrogenase. See (2) for method.

The PA method, and a scaled adjustment, designed to correct for the underestimation of CCS for large protein ions (3), were used to estimate the CCS of this clamp-loader homology model for comparison with its experimental CCS. A close agreement between the PA and measured CCS values was obtained, with a theoretical PA value of 10541 $Å^2$ for the model (see Fig. S3, yellow marker). Given that the PA underestimates CCS for protein ions, this hints at significant gas-phase structural collapse of the clamp loader. Indeed, the scaled PA value was found to be considerably larger than that measured at 11954 $Å^2$ (see Fig. S3, red marker).

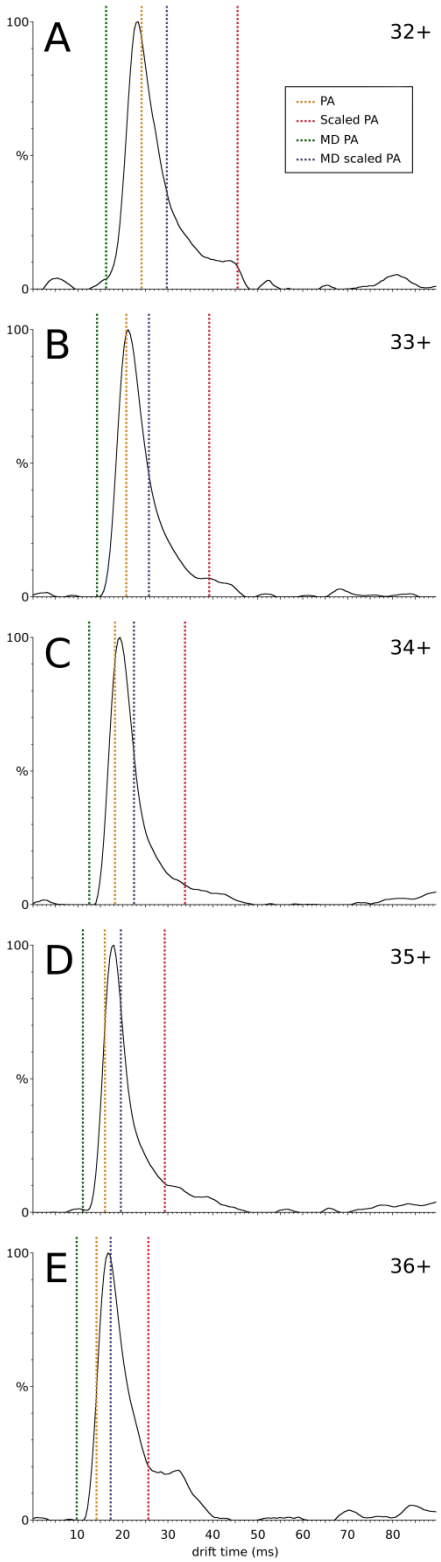

Figure S3. Plots of the drift time distributions obtained for 5 different charge states of the *Bacillus subtilis* clamp-loader complex by ion mobility and comparison with the homology model PA and scaled PA CCS values (orange and red markers, respectively), and the gas-phase MD PA and scaled PA values (green and blue markers, respectively). A, Charge state 32+. B, Charge state 33+. C, Charge state 34+. D, Charge state 35+. E, Charge state 36+.

In order to assess the degree of post-desolvation collapse a gas phase structure of the clamp-loader complex was generated by molecular dynamics (MD) simulation using the Amber99SB force field. The

resulting τ_3-δ-δ' structure showed a reduction in CCS of 8 %, bringing the scaled PA value (10967 $Å^2$) considerably closer to the experimental CCS of 10623 $Å^2$ (34+, see Fig. S3, blue marker), whilst maintaining similar architecture. We conclude from this that the *Bacillus* clamp loader complex undergoes significant gas-phase collapse. Recently, Hall *et al.* (7) have shown that relatively low energy activation of protein complexes in the gas-phase can induce structural collapse, before the onset of unfolding at higher energies. To ascertain whether this was occurring in our case, IMS measurements were conducted on the clamp loader complex at a range of activation energies, but it was determined that the collision energy used to measure the above CCS values were well below the threshold to trigger the onset of collapse.

X-ray Crystallography.

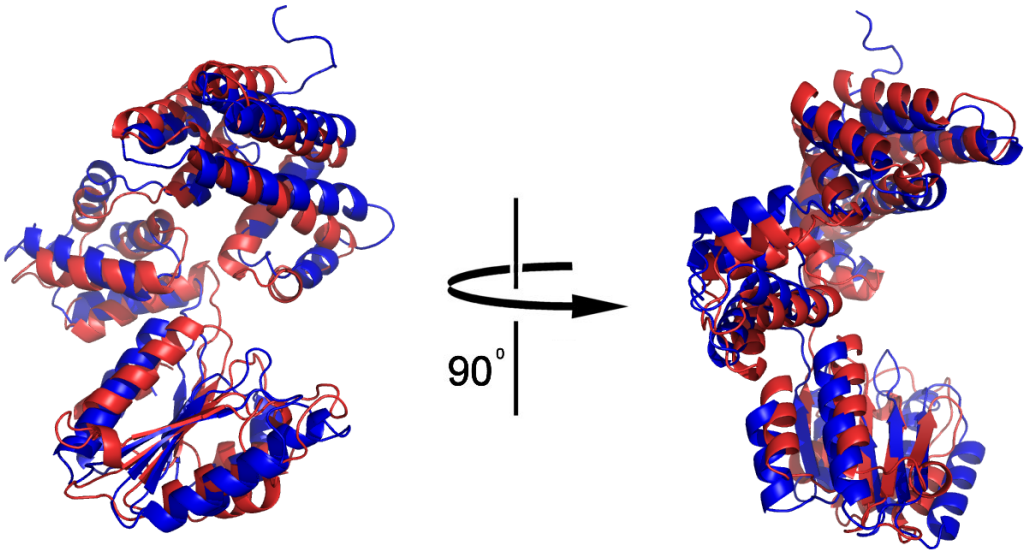

Figure S4 Superimposition of *B. subtilis* yqeN δ crystal structure (red) with the homology model of δ (blue) showing the close structural similarities (RMSD 4.6 Å for 329 Cα positions) and accuracy of the model.

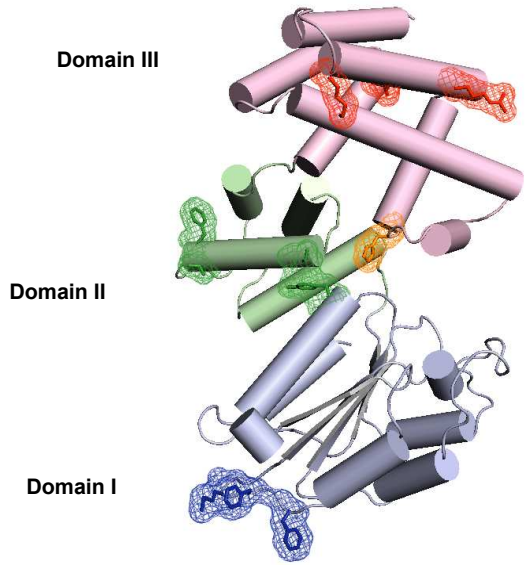

Figure S5 The crystal structure of *B. subtilis* yqeN (δ). Cartoon representation of the overall structure of yqeN. Domain I (res. 1 – 143), Domain II (res. 144 – 214) and Domain III (res. 215 – 339) are coloured pale blue, pale green and pink, respectively. The residues believed likely to interact with the β-clamp, τ (*dnaX*), δ' (*holB*) or the DNA are highlighted in blue, green, red and orange, respectively.

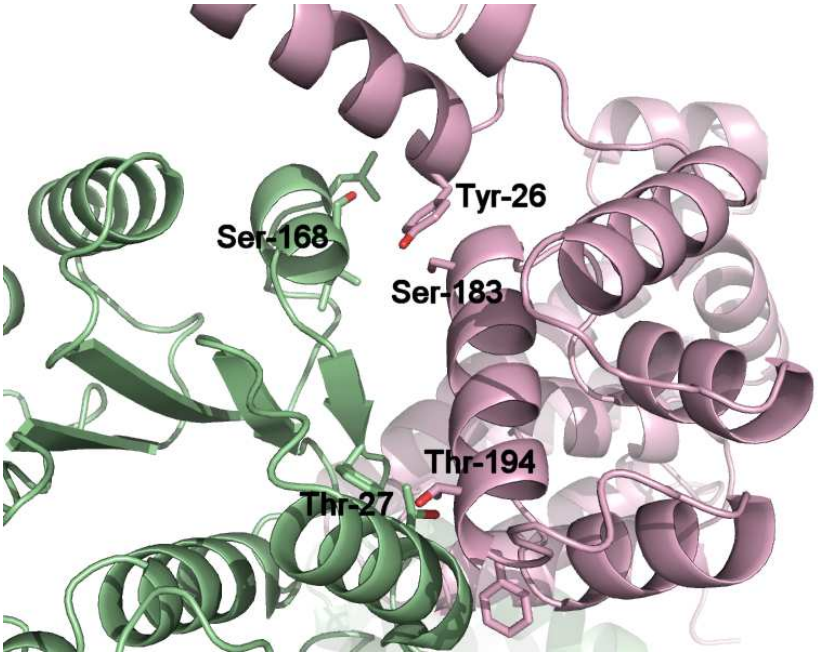

Figure S6 Predicted interface region for the δ-τ_3 interaction from the *B. subtilis* clamp loader homology model (δ model shown in pink, and τ model in green).

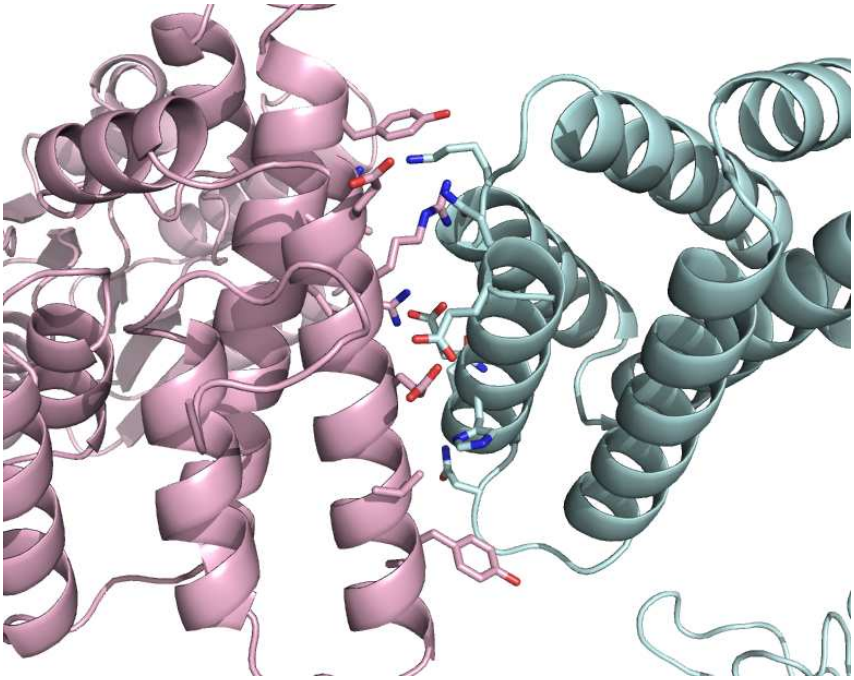

Figure S7 Predicted interface region for the δ-δ' interaction from the *B. subtilis* clamp loader homology model (δ model shown in pink, and δ' model in cyan).

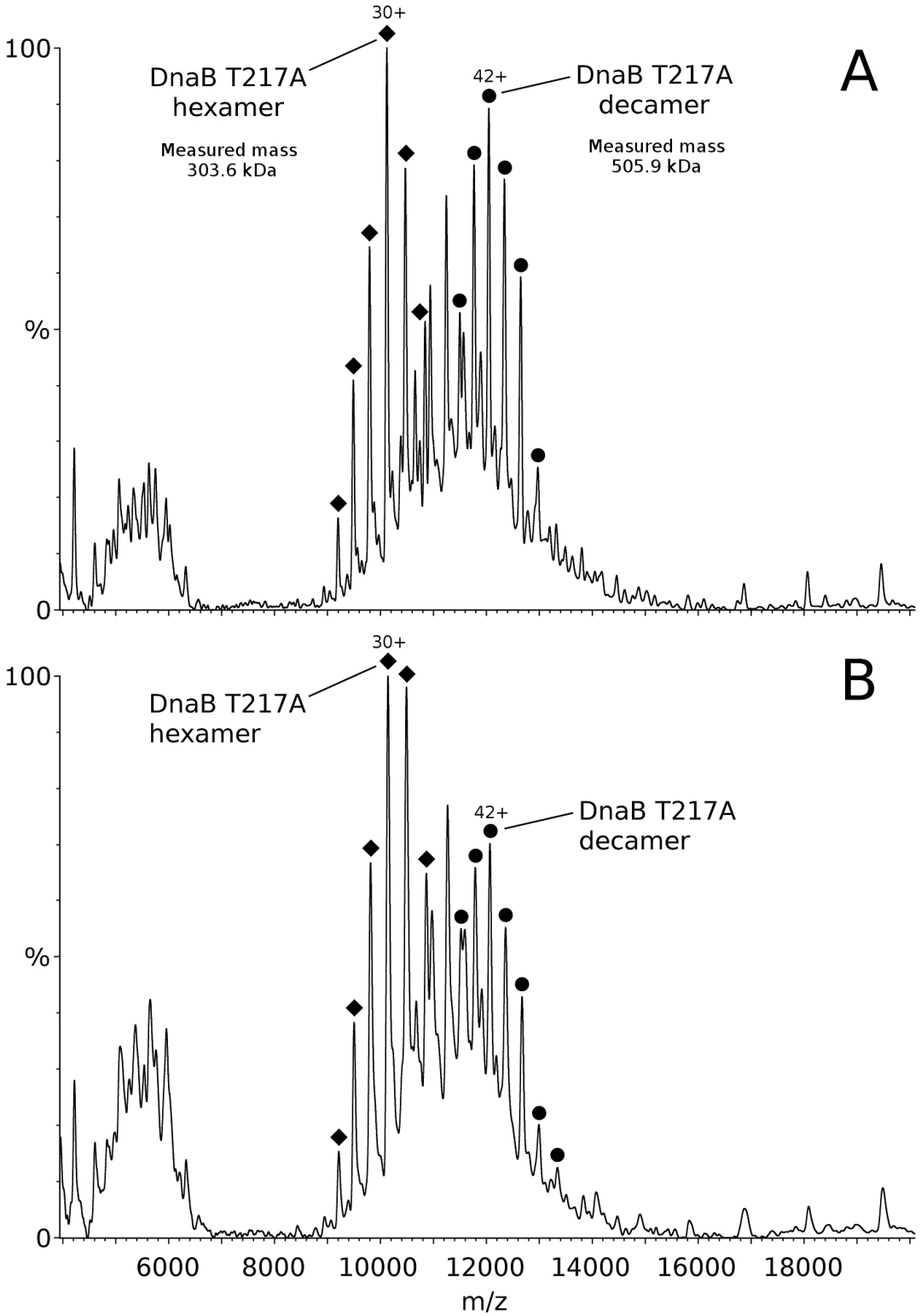

Figure S8 ESI-mass spectra of the *Bacillus subtilis* τ_3 subunit and the inactive *Bacillus stearothermophilus* Thr217Ala-DnaB helicase mutant from (A) is 1 M ammonium acetate only; and (B) 1 M ammonium acetate containing 500 uM Mg2+ and 100 uM ATP. No τ_3–DnaB mutant complex was observed in either case, demonstrating the requirement for ATP-fuelled conformational change in DnaB. Note: the T217A-DnaB mutant showed a significant amount of decamer as well as hexamer. The former stoichiometry also is seen in wild type-DnaB, but to a lesser extent (see Fig 4 in the main article).

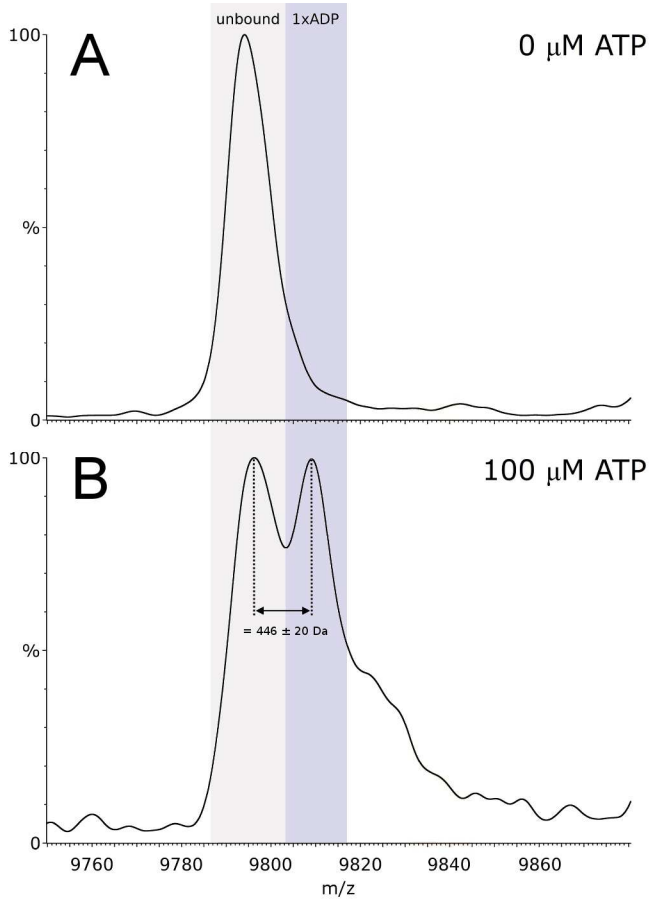

Figure S9 ESI mass spectra of 2 μM DnaB hexamer (+31 charge state shown) with (A) no added Mg^{2+}/ATP and (B) 500 μM and 100 μM ATP. The mass shift corresponds to one molecule of ADP (as the ammonium salt), indicating the hydrolysis of a single ATP is sufficient to induce conformational change and promote interaction with τ_3.

References

1. Bush, M. F., Hall, Z., Giles, K., Hoyes, J., Robinson, C. V., and Ruotolo, B. T. (2010) Collision Cross Sections of Proteins and their Complexes: a Calibration Framework and Database for Gas-Phase Structural Biology. *Anal. Chem.* **82**, 9557-9565.
2. Ruotolo, B. T., Benesch, J. L. P., Sandercock, A. M., Hyung, S.-J., and Robinson, C. V. Ion Mobility-Mass Spectrometry Analysis of Large Protein Complexes. (2008) *Nat. Protoc.* **3**, 1139-1152.
3. Bush, M. F., Hall, Z., Politis, A. Barsky, D., and Robinson, C. V. (2011) *59th Annual Conf. Amer. Soc. Mass Spectrom.* Denver, USA, WOB 2:50.
4. Amber on the eNMR Grid - a central resource funded by the European Union FP7 http://py-enmr.cerm.unifi.it/access/index.
5. Ritchie, D. W., and Venkatraman, V. (2010) Ultra-fast FFT protein docking on graphics processors. *Bioinformatics* **26**, 2398-2405.
6. The PyMOL Molecular Graphics System, Schrödinger, LLC.
7. Hall, Z. Politis, A. Bush, M. F. Smith, L. J. Robinson, C. V. (2012) Charge-State Dependent Compaction and Dissociation of Protein Complexes – Insights from Ion Mobility and Molecular Dynamics *J. Am. Chem. Soc.* **134**, 3429–3438.